

# THE EFFECT OF CARBON NANOTUBES ON THE SINTERING BEHAVIOR OF ZIRCONIA BASED MATERIALS

A. M. Zahedi, H. R. Rezaie\* and J. Javadpour

\* hrezaie@iust.ac.ir

Received: July 2015

Accepted: September 2015

School of Metallurgy and Materials Engineering, Iran University of Science and Technology (IUST), Tehran, Iran.

**Abstract:** Different volume fractions (1.3, 2.6, and 7.6 Vol.%) of carbon nanotubes (CNTs) were dispersed within 8Y-TZP nanopowders. Mixed powder specimens were subsequently processed by spark plasma sintering (SPS) and effects of CNTs on the sintering process of 8Y-TZP/CNT composites was studied. Maintenance of CNTs through the SPS process was confirmed using TEM and Raman Spectroscopy. Studies on the sintering profile of zirconia-CNT composites (Z-xC composites) could, to some extent, clarify the effect of CNTs' volume fraction on the densification rates of Z-xC composites. The specimen with the highest content of CNT (Z-7.6C) showed the lowest sintering rate while it was unable to reach full density.

**Keywords:** Sintering, Composites, Mechanical properties, ZrO<sub>2</sub>.

## 1. INTRODUCTION

Ceramic matrix composites (CMCs) have been the subject of several research works due to their excellent physical and mechanical properties. That leads these materials to be regarded as promising candidates for industrial applications [1-7]. This class of materials not only presents the common characteristics of a ceramic such as low weight, but also offers higher resistance against crack propagation (fracture toughness) [1,8,9].

The great interest in the incorporation of carbon nanotubes (CNTs) into the ceramic materials is a result of their extraordinary functional properties such as a high aspect ratio and excellent stiffness [10-13]. A proper dispersion of CNTs within the ceramic matrix should be known as the primary step in production of a successful CMC-CNT composite. This should be followed by an appropriate consolidation method with a little amount of damage on CNTs [14-19].

Field assisted/spark plasma sintering (SPS) is considered as a promising method to produce tailored ceramic composites with retained CNTs [20-23]. Such an approach is based on applying a pulsed electric current and consequently a lower sintering temperature combined with a shortened heating profile [24-27].

Milsom et al. studied sintering and grain growth mechanisms of spark-plasma-sintered

zirconia-CNT composites [28]. They have realized that CNTs would act as a kind of sintering aid to enhance densification and grain refinement. Mazaheri and his colleagues [10,23], on the other hand, have reported the transition of densification mechanisms of the ceramics to the higher temperatures in the presence of CNTs. They suggest that the flexibility of carbon nanotubes allows them to bend and pass through spaces between nanopowders and wrap around them.

The aim of the current investigation is to realize how varied fractions of CNTs would influence sintering behavior and grain growth of the processed zirconia-CNT (Z-xC) composites.

## 2. EXPERIMENTAL PROCEDURES

In the current investigation, 8mol% yttria stabilized zirconia (8YSZ) powder (Tosoh Co., Japan, Purity: > 99.7%) Mean particle size: 150 nm) as well as multi-walled carbon nanotubes (Arkema, France) were used as starting materials. The Multi walled carbon nanotubes are the commercially available grade of Graphistrength C-100, with the length of around 20 μm and a diameter of about 10–20 nm [12]. Figure 1 demonstrates visual studies performed on the raw materials. As can be observed, the mean particle size of zirconia powder is about 150 nm and the utilized CNTs are obviously bundled.

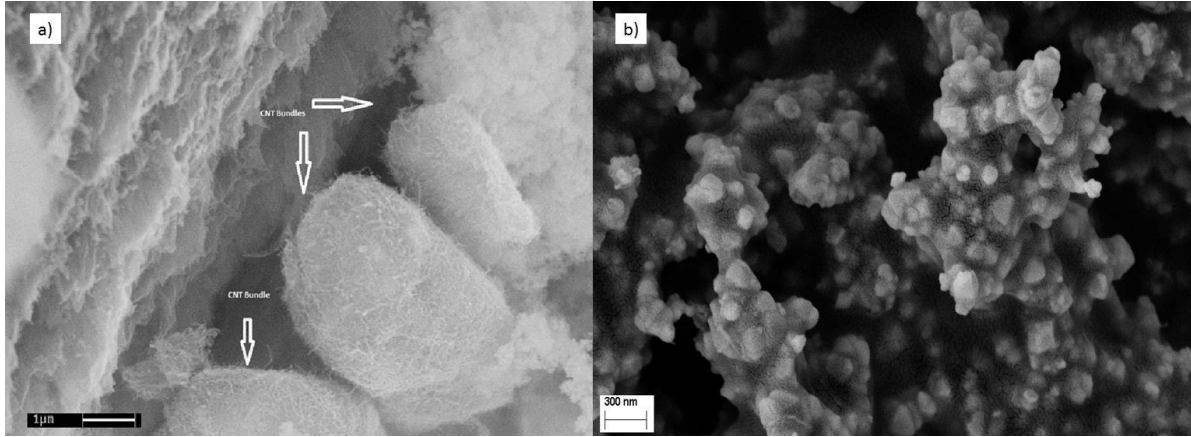


**Fig. 1.** CNTs bundles (a) and 8Y-TZP nanopowders (b) used in the current research.

Varied volume fractions of CNTs (0, 1.3, 2.6 and 7.6 Vol.%) were distributed within the matrix of 8Y-TZP nanopowder. Dispersion of CNTs was primarily carried out in an ethanol media using bath ultrasonication for 120 minutes and probe ultrasonication (heilscher, UP400s, Power: 400W, Frequency: 24KHz, Pulse: 0.5s) for 2 minutes. The process was subsequently followed by introducing the zirconia powder into the dispersed CNT solution. The powder mixture was then subjected to attrition milling in a medium of

ethanol with zirconia balls for 36 h. In order to produce fully dense composites and avoid nanotube damages, the specimens were consolidated using spark plasma sintering (SPS, FCT GmbH, Germany) under vacuum (0.007 bar) at different sintering temperatures of 1200, 1350 and 1400°C. The pressure applied during the process was maintained at 50 MPa and the soaking time was in the range of 5 to 20 min. The heating rate was 15 and 50 K.min<sup>-1</sup> based on the purpose of each test. Instantaneous measurement

**Table 1.** Details of the compositions, sample codes, and sintering characteristics of the specimens

| Composition        | Sample Code | Sintering Temperature (°C) | Green Density (%) | Sintered Density(%) |
|--------------------|-------------|----------------------------|-------------------|---------------------|
| Monolithic 8YSZ    | Z-0C        | 1200 °C                    | 49                | 93.2                |
| Monolithic 8YSZ    | Z-0C        | 1350 °C                    | 46                | 100                 |
| 8YSZ + 1.3Vol.%CNT | Z-1.3C      | 1200 °C                    | 52                | 95.5                |
| 8YSZ + 1.3Vol.%CNT | Z-1.3C      | 1350 °C                    | 46.4              | 99.7                |
| 8YSZ + 2.6Vol.%CNT | Z-2.6C      | 1200 °C                    | 48                | 92                  |
| 8YSZ + 2.6Vol.%CNT | Z-2.6C      | 1350 °C                    | 46.5              | 98.7                |
| 8YSZ + 7.6Vol.%CNT | Z-7.6C      | 1200 °C                    | 47                | 88.2                |
| 8YSZ + 7.6Vol.%CNT | Z-7.6C      | 1350 °C                    | 45                | 97.5                |

of relative density during the SPS process was performed by measuring the height variation of powder body, using related equations [23]. Details of the specimens and green/sintered density of the samples are presented in Table 1.

Density of sintered samples was measured using Archimedes method while theoretical densities of the composites were calculated based on the rule of mixtures. Accordingly, density of graphite ( $2.25 \text{ g.cm}^{-3}$ ) was used for CNT in the calculations and density of 8YSZ powder was assumed to be  $5.9 \text{ g.cm}^{-3}$ . Each data point was an average value of at least 10 measurements. The grain size of the samples was measured using the linear intercept method with a correction factor of 1.56 (LINCE, TU Darmstadt 2.31d version). Sample preparation for this analysis included a preliminary polishing stage on SiC abrasive papers with grit P80 to P2500. Subsequently, the specimens were subjected to a thermal etching stage in a vacuum furnace at 1150, 1250, or 1300 °C for 20 min. Three SEM images were used to measure the grain size of each sample, and in each micrograph at least 50 grains were assessed to calculate the average value. Microstructural observations were carried out using FIB-SEM (AURIGA 60 FIB-SEM, Carl Zeiss, Germany) as

well as high-resolution transmission electron microscopy (HR-TEM, CM-200, Philips, Netherlands). Raman Spectroscopy (Dispersive Raman, Senterra (2009), Bruker, Germany) was exploited to characterize degree of damage to CNTs before and after the processing.

### 3. RESULTS AND DISCUSSION

Dispersion of carbon nanotubes within ethanol media can be seen in the TEM graph of Fig. 2a. As can be observed, CNT bundles (shown in Fig. 1a) were obviously detached to single nanotubes of carbon using ultrasonic bath and probe. The applied wet dispersion method was furthermore verified when unbundled CNTs were distributed within the 8Y-TZP powder. As shown by Fig. 2b, dispersion of 7.6 Vol.% of nanotubes is, to some extent, successful and CNTs are seen to pass through the particles and wrap around them.

In order to verify this further and observe the final microstructure of the spark-plasma-sintered specimen, fractured surface of the Z-7.6C sample is shown in Fig. 3. This micrograph demonstrates degree of CNTs' dispersion and evaluates expediency of the processing. The applied dispersion method, as can be observed, seems to

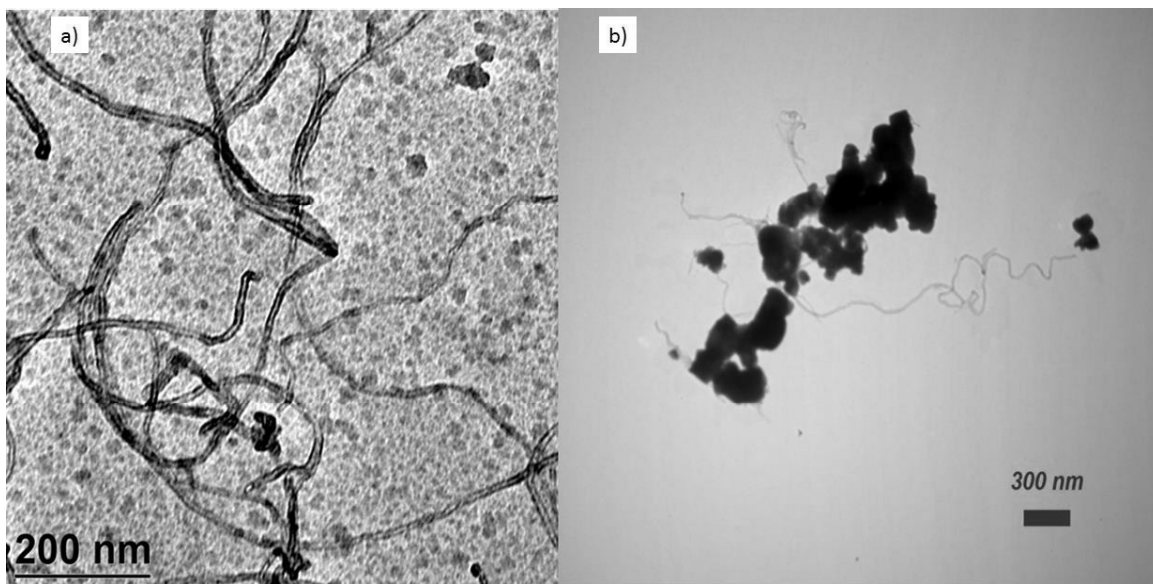
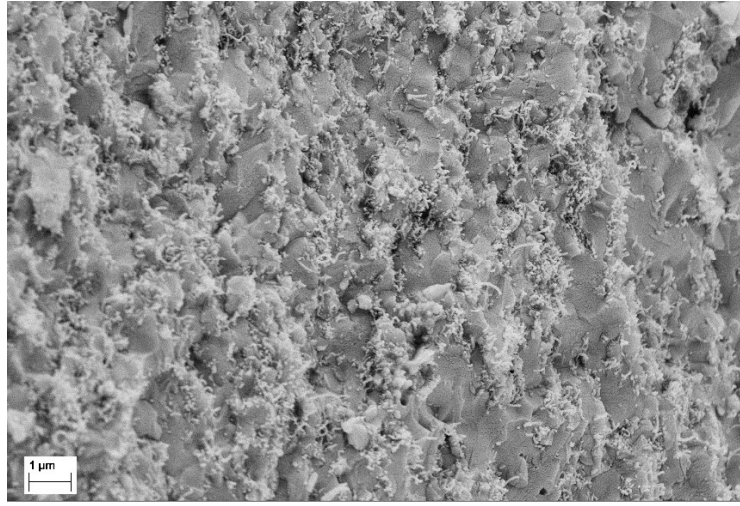


Fig. 2. Dispersed CNTs within ethanol (a) and dispersion of 7.6Vol.% CNTs within 8Y-TZP nanopowders (b).



**Fig. 3.** Fractured surface of the Z-7.6C sample sintered at 1350 °C.

have ended in a homogeneous distribution of CNTs within the microstructure of Z-7.6C sample. CNTs are well distributed through the whole surface and this figure should be appreciated as a clear evidence for success of the aforementioned wet dispersion.

As can be observed, CNTs are well detached from an entangled bundle and are seen to have wrapped around zirconia particles due to their flexible nature. Moreover, while CNTs are

appeared to be shortened through the processing stage, their walls seem to have experienced the least of damages. Such an assertion won further verifications by performing Raman spectroscopy as the most reliable apparatus to ensure safety and maintenance of CNTs. Fig 4a compares Raman Spectroscopy pattern of pure carbon nanotubes with as-sintered Z-7.6C sample. As can be observed, the characteristic peaks of CNTs in the sintered specimens are located in the closed

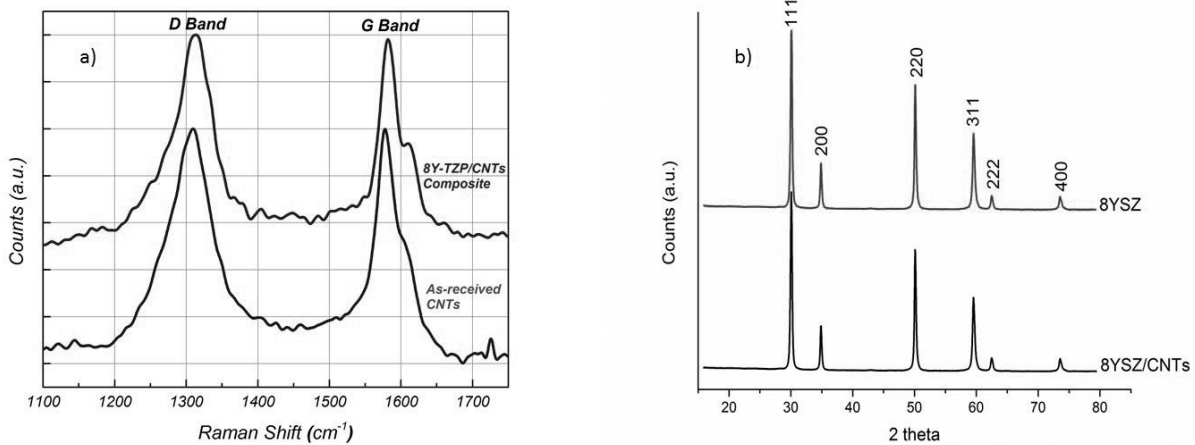


**Fig. 4.** Raman Spectra of as-received CNTs and as-sintered Z-7.6C composite (a) and X-ray diffraction pattern of 8YSZ nanopowders compared to the sintered Z-7.6C sample (samples have been sintered at 1350°C).

positions to those in pure CNTs. Moreover, calculation of ID/IG intensity ratio reveals a very slight increase after sintering. This factor is an evidence to evaluate degree of damages to CNTs through the processing stage and the higher this value, the greater is the damage to CNTs.

In order to investigate any probable interaction between CNTs and the matrix powder, Fig 4b presents a comparison between the X-ray diffraction pattern of the as-received 8Y-TZP nanopowders and the sintered Z-7.6C composite. One can hardly detect any transition in the peak positions after sintering of the composite powders. This certainly rules out probability of any new phase generation through the processing of specimens.

The above studies demonstrated the homogeneous distribution of carbon nanotubes through the exploited wet dispersion method and confirmed their maintenance after the SPS process. As a result, wet dispersion followed by the SPS process was adopted as the basic profile in the current work.

Subsequently, sintering behavior of Z-xC composites was studied using 8Y-TZP powder incorporated with 0, 1.3, 2.6 and 7.6 vol.% of carbon nanotubes. Fig 5a plots relative density of Z-xC composites as a function of temperature.

As reported in the literature, CNTs are expected to retard densification of composites and the higher CNT volume fraction, the slower densification rates. Such a behavior was also approved in this study and the sample with the highest volume fraction of CNTs (Z-7.6C) showed the lowest final density. While the monolithic sample reached full densification, Z-7.6C specimen could hardly attain relative density of higher than 0.97. Such a trend was also confirmed by Z-2.6C composite and the related curve to this specimen was normally located below the monolithic sample. The remaining issue referred to Z-1.3C sample which finally showed a relative density of higher than 0.99. As can be seen in figure 5a, Z-1.3C composite experienced a higher density in the entire SPS process, except at the very final stage of sintering. As mentioned earlier, CNTs are normally expected to degrade densification process and the composite samples have been reported [8-12] to endure a constraint sintering in the presence of rigid inclusions. Thereupon, in order to find an answer for the behavior of Z-1.3C samples, the specimens were sintered at 1200 °C, in which Z-xC composites could undergo an extended densification time through the isothermal stage of SPS. Fig 5b displays sintering rate of Z-xC composites versus the relative density at the isothermal stage of

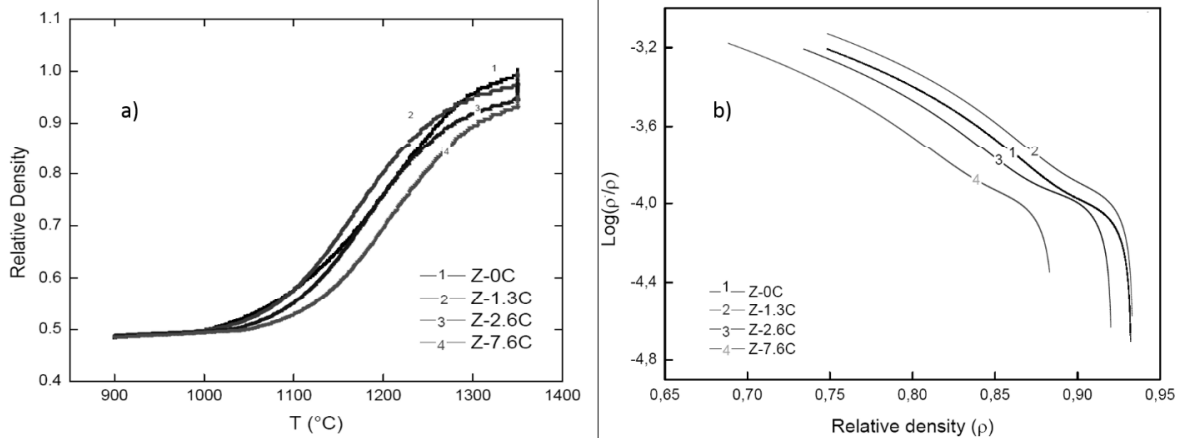


**Fig 5.** Relative density of Z-xC composites sintered by SPS at 1350 °C for 10 min vs. Temperature (a) and sintering rate of Z-xC composites sintered by SPS at 1200 °C for 20 min vs. relative density (b).

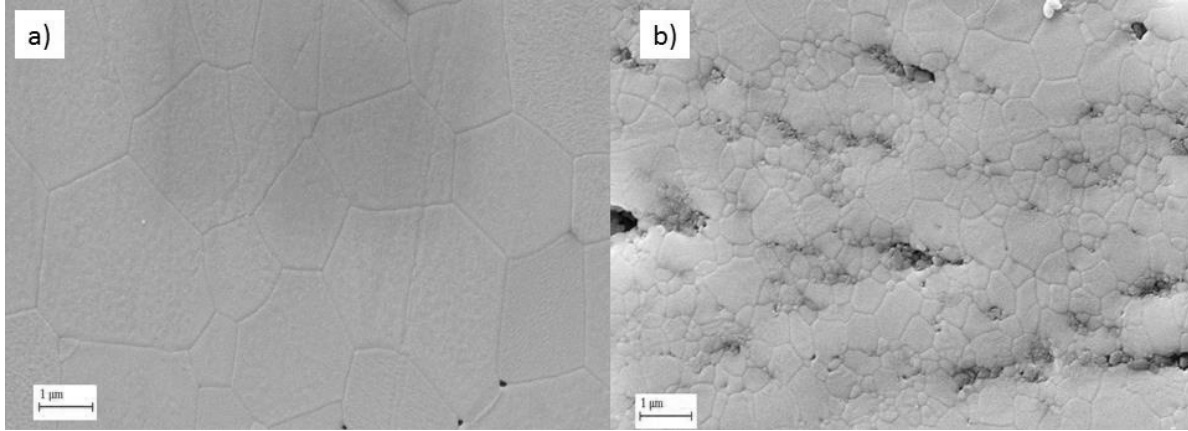


**Fig. 6.** SEM micrographs of Z-0C (a) and Z-7.6C (b) samples sintered at 1400 °C for 10 minutes.

sintering (1200 °C). As can be seen, results of the previous figure are to a large extent confirmed by these graphs where the specimen with the highest fraction of CNTs (Z-7.6C) showed the lowest densification rate. Z-1.3C sample, on the other hand, revealed the highest sintering rates among Z-xC specimens. That can be considered as solid evidence of verifying the results of Fig 5a where Z-1.3C sample had shown an enhanced densification trend compared to the monolithic material (Z-0C). Detailed explanations around the superior densification rate of the specimen with the lowest fraction of CNTs (Z-1.3C) can be found in another publication by the current authors [29]. However, what should be taken into account is that the very well-known effect of CNTs in degradation of sintering rates is more highlighted when the volume fraction of CNTs trespasses a critical point. This critical content is not precisely determined and may be associated with the quality of dispersion. However, what is clear is that, below the aforementioned critical content, CNTs can impart positive effects on the densification of CNT incorporated composites. Such an observation has been previously reported by Milsom et al. [28] where they explained that addition of 0.5 and 2 vol% CNTs into zirconia matrix resulted in an enhanced densification behavior compared to the monolithic zirconia. Positive effect of nanotubes in improving superplastic behavior of alumina matrix has been

discussed by another investigation [30]. They suggest that CNTs exert a lubricating type of effect throughout the sintering process and would ease sliding of the matrix's grains on the boundaries. Such an effect is, undoubtedly, expectable when the volume fraction of nanotubes is below the critical point (around 0 to 1.5vol%), after which, nanotubes, specifically, in case of a poor dispersion would entangle and impose constraining effects on the system.

One of the major effects proposed by CNTs refers to their grain growth suppression of CNT containing composites. Figs. 6 a and b demonstrate the SEM micrographs of Z-0C and Z-7.6C specimens, respectively. Both samples have been sintered at 1400 °C for 10 minutes and attained relative density of 1 and 0.97 T.D, respectively. The main point within this figure is the role that CNTs play to inhibit an accelerated grain growth in Z-7.6C composite compared to the pure zirconia. Microstructural analysis of the figures reveals a 5 time larger grain size for Z-0C sample compared to Z-7.6C. This implies the effect of CNTs on the microstructural variations of the composites. In particular, CNTs possess a competence to wrap around the grains and prevent the accelerated grain growth at the final stages of sintering [8-12].

#### 4. CONCLUSION

In the current investigation, carbon nanotubes (0, 1.3, 2.6, and 7.6 Vol.%) were dispersed within 8Y-TZP powder. Spark plasma sintering (SPS) was exploited to produce 8Y-TZP/CNT composites with varied range of CNTs' content (Z-xC, x=CNTs' volume fraction). The specimens were found to attain the maximum of sintered density at 1350 °C and the sample with the highest amount of CNTs was unable to reach near full density. CNTs were found to degrade sintering rate of the composites and densification seemed to be more and more blocked with increasing CNTs' fraction. The only deviation from this expectation was seen when Z-1.3C sample (composite with the lowest CNTs' content) showed a higher sintering rate compared to the monolithic material. The effect of carbon nanotubes on the grain refinement of Z-xC composites was also studied. While the monolithic sample was found to experience an accelerated grain growth at the final sintering stages, the addition of CNTs could hinder the grain growth and resulted in a finer microstructure in Z-7.6C composite.

#### 5. ACKNOWLEDGMENT

The authors of the paper express their gratitude to Dr. M. Mazaheri and Mr. M. Taheri due to their valuable services during the course of this research. Financial and scientific supports offered by the group of Mechanics of Functional Materials in Friedrich Schiller University of Jena are also appreciated.

#### REFERENCES

1. Zapata-Solvas, E., Gomez-Garcia, D. and Dominguez-Rodriguez, A., "Towards physical properties tailoring of carbon nanotubes-reinforced ceramic matrix composites", *J. Eur. Ceram. Soc.*, 2012, 32, 3001–3020
2. Robinson, A. L., "An oxygen key to the new superconductors". *Science*, 1987, 236, 1063–5.
3. Scott, J. F. and Araujo, C. A. P., "Ferroelectric memories". *Science* 1989, 246, 1400–1405.
4. Padture, N. P., Gell, M. and Jordan, E. H., "Thermal barrier coatings for gas-turbine engine applications". *Science*, 2002, 296, 280–284.
5. Jayaseelan, D. D., Zapata-Solvas, E., Brown, P. and Lee, W. E., "In situ formation of oxidation resistant refractory coatings on SiC-reinforced ZrB<sub>2</sub> UHTCs". *J. Am. Ceram. Soc.* 2012, 95, 1247–1254.
6. Hogg, P. J., "Composites in armor". *Science*, 2006, 314, 1100–1101.
7. Wentorf, R. H., Devries, R. C. and Bundy, F. P., "Sintered superhard materials", *Science*, 1980, 208, 873–880.
8. Taheri, M., Mazaheri, M., Golestani-fard, F., Rezaie, H. R. and Schaller, R., "High/room temperature mechanical properties of 3Y-TZP/CNTs composites", *Ceram. Int.*, 2014, 40, 3347–3352.
9. Mazaheri, M., Mari, D., Razavi-Hesabi, Z., Schaller, R. and Fantozzi, G., "Multi-walled carbon nanotube/nanostructured zirconia composites: Outstanding mechanical properties in a wide range of temperature", *Compos. Sci. Technol.*, 2011, 71, 939–945.
10. Mazaheri, M., Mari, D. and Schaller, R., "High temperature mechanical spectroscopy of yttria stabilized zirconia reinforced with carbon nanotubes", *Phys. status solidi (a)*, 2010, 207, 2456-2460.
11. Mazaheri, M., Mari, D., Schaller, R. and Fantozzi, G., "High Temperature Mechanical Spectroscopy Study of 3 mol% Yttria Stabilized Tetragonal Zirconia Reinforced with Carbon Nanotubes", *Sol. ST. Phen.*, 2012, 184, 265-270.
12. Mazaheri, M., "High Temperature Behavior of Nano-Structured Ceramic Composites Studied by Mechanical Spectroscopy", PhD, Laboratoire de Physique de la Matière Complexe (LPMC), Ecole Polytechnique Fédérale de Lausanne (EPFL), 2012.
13. Mukhopadhyay, A., Chu, B. T. T., Green, M. L. H. and Todd, R. I., "Understanding the mechanical reinforcement of uniformly dispersed multiwalled carbon nanotubes in alumino-borosilicate glass ceramic", *Acta Mater.*, 2010, 58, 2685-2697.
14. Peng-Cheng M., Siddiqui, N. A., Marom, G. and Kim, J. K., "Dispersion and functionalization of carbon nanotubes for

- polymer-based nanocomposites”, *Composites: Part A*, 2010, 41, 1345–1367.
15. Hilding, J., Grulke, E. A., George-Zhang, Z., and Lockwood, F., “Dispersion of Carbon Nanotubes in Liquids”, *Journal of Dispersion Science and Technology*, 24, 2003, 1–4.
  16. Vaisman, L., Wagner, H. D. and Marom, G., “Advances in Colloid and Interface Science”, 2006, 37–46, 128–130.
  17. Huang, Y. Y. and Terentjev, E. M., “Dispersion of Carbon Nanotubes: Mixing, Sonication, Stabilization, and Composite Properties”, *Polymers* 4, 2012, 275-295.
  18. O’Brien, N. P., McCarthy, M. A. and Curtin, W. A., “Improved inter-tube coupling in CNT bundles through carbon ion irradiation”, *carbon* 51, 2013, 173–184
  19. Peigney, A., Laurent, C. H., Flahaut. E., Bacsu, R. R., Rousset, A., “Specific surface area of carbon nanotubes and bundles of carbon nanotubes”, *Carbon* 39, 2001, 507–514.
  20. Cho, J., Boccaccini, A. R., Shaffer, M. S. P., “Ceramic matrix composites containing carbon nanotubes”, *Journal of Materials Science*, 2009, 44, 1934–1951.
  21. Inama, F., Peijs, T., and Reece, M. J., “The production of advanced fine-grained alumina by carbon nanotube addition”, *Journal of the European Ceramic Society* 31, 2011, 2853–2859.
  22. Huang, Q., Jiang, D., Ovid’ko, I. A., and Mukherjee, A., “High-current-induced damage on carbon nanotubes: The case during spark plasma sintering”, *Scripta Materialia* 63, 2010, 1181–1184.
  23. Mazaheri, M., Mari, D., Schaller, R., Bonnefont, G. and Fantozzi, G., “Processing of yttria stabilized zirconia reinforced with multi-walled carbon nanotubes with attractive mechanical properties”, *Journal of the European Ceramic Society* 31, 2011, 2691–2698.
  24. Shen, Z., Johnsson, M., Zhao, Z., and Nygren, M., “Spark Plasma Sintering of Alumina”, *Journal of American Ceramic Society*, 2002, 85, 1921–27.
  25. Demuynecka, M., Erauwa, J. P., Van der Biest, O., Delannay, F., Cambier, F., “Densification of alumina by SPS and HP: A comparative study”, *Journal of the European Ceramic Society* 32, 2012, 1957–1964.
  26. Grasso, S., Sakka, Y., and Maizza, G., “Electric current activated/assisted Sintering (ECAS): a review of patents 1906–2008”, *Science and Technology in Advanced Materials* 10, 2009, 053001 (24).
  27. Garay, J. E., “Current-Activated, Pressure-Assisted Densification of Materials, *Materials Science and Engineering Program*”, Department of Mechanical Engineering, University of California, Riverside, California 92521.
  28. Milsom, B., Viola, G., Gao, Z., Inam, F., Peijs, T., Reece, M. J., “The effect of carbon nanotubes on the sintering behaviour of zirconia”, *Journal of the European Ceramic Society* 32, 2012, 4149–4156.
  29. Zahedi, A. M., Gonzalez, J., Mazaheri, M., Javadpour, J., Rezaie, H. R., Guillon, O., “Field-Assisted/Spark Plasma Sintering Behavior of CNT-Reinforced Zirconia Composites: A Comparative Study between Model and Experiments, *Journal of the European Ceramic Society*”, 35, 2015, 4241-4249.
  30. Huang, Q., Bando, Y., Xu, X., Nishimura, T., Zhi, C., Tang, C., Xu, F., Gao, L. and Golberg, D., “Enhancing superplasticity of engineering ceramics by introducing BN nanotubes”, *Nanotechnology*, 18, 2007. 485-706.